Fractal Fragmentation, Soil Porosity, and Soil Water Properties: I. Theory

Michel Rieu* and Garrison Sposito

ABSTRACT

Recent efforts to characterize soil water properties in terms of porosity and particle-size distribution have turned to the possibility that a fractal representation of soil structure may be especially apt. In this paper, we develop a fully self-consistent fractal model of aggregate and pore-space properties for structured soils. The concept underlying the model is the representation of a soil as a fragmented fractal porous medium. This concept involves four essential components: the mathematical partitioning of a bulk soil volume into self-similar pore- and aggregate-size classes, each of which is identified with a successive fragmentation step; the definition of a uniform probability for incomplete fragmentation in each size class; the definition of fractal dimensions for both completely and incompletely fragmented porous media; and the definition of a domain of length scales across which fractal behavior occurs. Model results include a number of equations that can be tested experimentally: (i) a fractal dimension ≤ 3; (ii) a decrease in aggregate bulk density (or an increase in porosity) with increasing aggregate size; (iii) a power-law aggregate-size-distribution function; (iv) a water potential that scales as an integer power of a similarity ratio; (v) a power-law expression for the water-retention curve; and (vi) an expression for hydraulic conductivity in terms of the conductivities of single-size arrangements of fractures embedded in a regular fractal network. Future research should provide experimental data with which to evaluate these predictions in detail.

THE STRUCTURE OF SOIL and its close relationship to aeration and water movement have been studied intensively by soil physicists throughout the present century (Hillel, 1980, Ch. 6). Of perhaps most importance in these studies is the characterization of the soil fabric and its associated pore space (Kemper and Rosenau, 1986; Danielson and Sutherland, 1986).

This classic problem in soil physics recently has taken on new dimensions with the recognition that, because soil is both a fragmented material and a porous medium, a fractal representation may be especially appropriate (Mandelbrot, 1983; Turcotte, 1986; Feder, 1988). Fractal representations of soils as fragmented materials produced by weathering processes have been developed in a variety of ways during the past 20 yr, usually based on a power-law distribution function for particle size (Hartmann, 1969; Turcotte, 1986, 1989). Similar fractal representations of colloidal media have been derived on the basis of assumptions about the physics of aggregate growth (Jullien and Botet, 1987; Schaefer, 1989). Fractal representations of sediments as porous media also are abundant in the literature (see, e.g., the review by Thompson et al. [1987]) and, very recently, Tyler and Wheatcraft (1989, 1990) have described fractal models of soil that relate particle-size distribution to pore-size distribution, and thus to soil water properties. As noted by Arya and Paris (1981), Saxton et al. (1986), and Haverkamp and Parlange (1986), laboratory or field measurements of the relation between water potential and water content, and the relation between hydraulic conductivity and either water potential or water content, are time consuming and expensive. For this reason, studies often have been carried out using an alternative procedure, which consists of predicting soil water properties from simpler, routine laboratory measurements of soil bulk density or particle-size distribution (Cosby et al., 1984; Saxton et al., 1986). Arya and Paris (1981) have presented an exhaustive review of different models that have been developed for use in this approach, and they have described a physical model of soil porosity based on the particle-size distribution. In their model, the relation between pore radius and particle radius involves an exponent that has been interpreted recently through a fractal concept by Tyler and Wheatcraft (1989). In a similar vein, Haverkamp and Parlange (1986) considered a constant packing parameter that relates pore and particle radii, suggesting that pores of different sizes were nonetheless similar in shape. Tyler and Wheatcraft (1990) have suggested that this similarity, interpreted with fractal concepts, is basic to the commonly observed power-law relationships among soil water properties.

We have developed a general theoretical framework for a self-consistent fractal representation of soil as both a fragmented natural material and a porous medium. We began with a description of virtual pore-size fractions in a porous medium, motivated by an approach of Childs and Collis-George (1950), that permits a facile introduction of fractal concepts of the solid matrix and pore space. These concepts led to equations for the porosity and bulk density of both the size fractions and the porous medium in terms of a characteristic fractal dimension, D. The equations derived apply to materials that have been fragmented into a collection of unconnected aggregates, such as occurs in particle-size analysis. The aggregate-size distribution for this collection follows a power-law expression involving D. The fractal representation was then extended to describe a structured field soil whose aggregates are interconnected by solid material to form a stable pore space. Using a concept of incomplete fragmentation of a fractal porous medium (Turcotte, 1986, 1989), we derived equations for the porosity and bulk density that involve a "bulk" fractal dimension, D_r. These equations can be tested with suitable experimental measurements on the structure and porosity of natural soils. Once a fractal, incompletely fragmented structure is described for a soil, its pore space can be represented by conducting network of similar, size-scaled fractures and it is possible to derive testable relationships among soil water content, water potential, and hydraulic conductivity.

Michel Rieu, Centre ORSTOM Bondy, 70-74 Route d'Aulnay, 93143 Bondy Cédex, France; Garrison Sposito, Dep. of Soil Science, Univ. of California, Berkeley, CA 94720. Received 12 Feb. 1990. *Corresponding author.

Published in Soil Sci. Soc. Am. J. 55:1231–1238 (1991).

FRACTAL STRUCTURE AND POROSITY

Virtual Pore-Size Fractions

Consider a porous medium whose porosity results from a broad range of pore sizes, decreasing in mean (or median) diameter from p_o to p_{m-1} ($m \geq 1$). A bulk element of the porous medium, of volume V_o large enough to include all sizes of pore, has porosity ϕ and the dry bulk density σ_o. Following Childs and Collis-George (1950), we shall divide the pore-volume distribution of V_o mathematically into m virtual pore-size fractions, with the ith *virtual size fraction* defined by

$$P_i \equiv V_i - V_{i+1} \qquad (i = 0, \ldots, m-1) \qquad [1]$$

where P_i is the volume of pores solely of size p_i contained in V_i, the ith *partial volume* of the porous medium, which itself contains all pores of size $\leq p_i$. The partial volume V_{i+1} thus is contained in V_i and the partial volume V_{m-1} contains the smallest pore-size fraction, P_{m-1}, along with the *residual solid volume*, denoted V_m. In general, the solid material whose volume is V_m will not be chemically or mineralogically homogeneous. Its mass density, denoted σ_m, is thus an average "primary particle" density. Given Eq. [1], the bulk volume of the porous medium can be represented mathematically as the sum of m increments of the virtual pore-size fraction P_o to P_{m-1}, plus a residual solid volume V_m:

$$V_o = \sum_{i=0}^{m-1} P_i + V_m \qquad [2]$$

Successive increments of pore volume P_i are ratioed to the corresponding partial volumes V_i to define the *pore coefficient*:

$$\Gamma_i \equiv P_i/V_i \qquad (\Gamma_i < 1) \qquad [3]$$

or, using Eq. [1],

$$V_{i+1} = (1 - \Gamma_i)V_i \qquad (i = 0, \ldots, m-1) \qquad [4]$$

The pore coefficient Γ_i is interpreted as the partial porosity contributed to V_i by pores of size p_i. It follows from Eq. [4] that the residual solid volume V_m can be expressed

$$V_m = V_{m-1}(1 - \Gamma_{m-1}) \cdot \cdot \cdot = V_{m-j} \prod_{i=m-j}^{m-1} (1 - \Gamma_i) \quad \cdot \quad (j = 1, \ldots, m) \qquad [5]$$

where the second step comes from repeated application of Eq. [4]. The porosity of the medium then can be expressed as a product involving the pore coefficients:

$$\phi \equiv (V_o - V_m)/V_o \qquad [6]$$

$$= 1 - \prod_{i=0}^{m-1} (1 - \Gamma_i) \qquad [7]$$

where Eq. [5] has been inserted with j set equal to m. Equation [7] is a representation of the porosity as the difference between 1 and the product of successive partial-volume fractions, $V_{i+1}/V_i = 1 - \Gamma_i$.

Fractal Porous Media

A *fractal porous medium* is one in which there is self-similarity of both the pore space and the solid matrix (Mandelbrot, 1983, Ch. 14; Jullien and Botet, 1987, Ch. 3). In the context of Eq. [1], this means that both the increments of pore volume, P_i, and the partial volumes, V_i, are similar in shape and obey scaling relations in size. To introduce the scaling property, we define a *linear similarity ratio*, denoted r, which relates successive pore sizes p_i or successive partial volumes represented by their mean (or median) diameters d_i:

$$p_{i+1} = rp_i \qquad (r < 1) \qquad [8a]$$

$$d_{i+1} = rd_i \qquad (r < 1) \qquad [8b]$$

Corresponding to Eq. [8], the pore-volume increments and the partial volumes then scale as r^3:

$$P_{i+1} = r^3 P_i \qquad [9a]$$

$$V_{i+1} = r^3 V_i \qquad [9b]$$

which implies

$$P_i/V_i = \text{constant} = \Gamma \qquad (i = 0, \ldots, m-1) \qquad [10]$$

In a scaling porous medium the pore coefficients are uniform across all virtual pore-size fractions.

The self-similarity property of a fractal porous medium means that, for each virtual pore-size fraction, a constant number N of smaller volumes V_{i+1} (or P_{i+1}) can be associated with any volume V_i (or P_i) (Mandelbrot, 1983, Ch. 6). Simply put, every volume V_i contains N smaller volumes V_{i+1} and one associated pore volume P_i:

$$V_i \equiv NV_{i+1} + P_i \qquad (i = 0, \ldots, m-1) \qquad [11]$$

In turn, each volume V_{i+1} contains N volumes V_{i+2} and one associated pore volume P_{i+1}, and so on. Therefore, N pore volumes P_{i+1} can also be associated with each pore volume P_i and Eq. [2] takes the form

$$V_o = \sum_{i=0}^{m-1} N^i P_i + N^m V_m \qquad [12]$$

where now $N^m V_m$ represents the residual solid volume. Equation [4] becomes

$$V_{i+1}/V_i = (1 - \Gamma)/N \qquad (i = 0, \ldots, m-1) \qquad [13]$$

because of Eq. [10] and [11]. Equation [5] correspondingly is transformed to the expression

$$V_m = V_{m-j}(1 - \Gamma)^j N^{-j} \qquad (j = 1, \ldots, m) \qquad [14]$$

The porosity of the medium is then

$$\phi \equiv (V_o - N^m V_m)/V_o \qquad [15]$$

$$= 1 - (1 - \Gamma)^m \qquad [16]$$

after the insertion of Eq. [14] with j set equal to m. Similarly, the *partial porosity* ϕ_i of a partial volume V_i is defined by

$$\phi_i \equiv (N^i V_i - N^m V_m)/N^i V_i \qquad [17]$$

$$= 1 - (1 - \Gamma)^{m-i} \qquad (i = 0, \ldots, m-1) \qquad [18]$$

where Eq. [14] has been used with $j = m - i$ to obtain Eq. [18]. Equation [18] leads to the important result

that, in a fractal porous medium, the porosities of successive partial volumes decrease with the pore size, as the index i approaches m. The *fractal dimension* of a porous medium is defined by (Mandelbrot, 1983, p. 37)

$$D \equiv \log N/\log(1/r) \qquad (D > 0) \qquad [19]$$

where N appears in Eq. [11] and r is defined in Eq. [8]. The fractal dimension is related closely to the pore coefficient, Γ. This can be seen by combining Eq. [9b] and [13] to obtain the expression

$$\Gamma = 1 - Nr^3 \qquad [20]$$

which, with Eq. [19], leads to the result

$$\Gamma = 1 - r^{3-D} \qquad (\Gamma < 1, r < 1) \qquad [21]$$

Equation [21] shows that, in a fractal porous medium where pore sizes are scaled by the similarity ratio $r < 1$, the magnitude of the pore coefficient decreases as the fractal dimension increases. The relation between the porosity and the fractal dimension now follows from Eq. [16] and [21]:

$$\phi = 1 - (r^{3-D})^m \qquad [22]$$

For a given value of the exponent m, the porosity of a fractal porous medium decreases as the fractal dimension increases. Equation [22] shows further that *the fractal dimension of a porous medium must be <3.*

Natural porous media typically exhibit only a limited domain (or domains) of pore length scale across which fractal behavior is observed (Thompson et al., 1987; Turcotte, 1989), such that the index m always has a finite value. The upper and lower limits of this domain can be identified with the corresponding limits on the partial volume diameters d_o and d_m respectively. It follows from Eq. [8b] that

$$d_m/d_o = r^m \qquad [23]$$

and from Eq. [22] that

$$\phi = 1 - (d_m/d_o)^{3-D} \qquad [24]$$

The partial porosities ϕ_i also can be connected with partial volume diameters by combining Eq. [8b], [18], [21], and [23]:

$$\phi_i = 1 - (d_m/d_i)^{3-D} \qquad [25]$$

As $D \uparrow 3$, the ϕ_i become smaller, corresponding to a more finely partitioned porosity, whereas a small value of D results in a more coarsely partitioned porosity with larger ϕ_i for a given set of d_i. Thus, the fractal dimension can be interpreted to represent the partitioning of the porosity into size classes, with a larger fractal dimension representing a smaller, more finely partitioned porosity. If $3 - D$ is very small, Eq. [18] can be expanded in a MacLaurin series in Γ to show that $\phi_i \approx (m - i)\Gamma$ for the partial porosities in the limit of small pore coefficients.

FRAGMENTED FRACTAL POROUS MEDIA

Complete Fragmentation

The concepts of virtual pore-size fractions, pore coefficients, and porosity were developed in Eq. [1] through [7] without consideration of scaling or self-similarity. They apply to any porous medium with an arbitrary distribution of pore sizes (Fig. 1a). Equations [10] through [25] specialized these concepts (plus that of partial porosity) to a porous medium that exhibits scaling relations and self-similarity as defined by Eq. [8], [9], and [11]. A well-known example of this kind of fractal porous medium is the Menger sponge (Mandelbrot, 1983, p. 134), shown in Fig. 1b for the case $r = 1/3$, $N = 20$, $D = 2.7268$. The solid matrix and the pore space each form connected sets of similar elements. The volume P_i comprises a single rectangular pore in each partial volume V_i and the pore space itself comprises size-scaled, similar pores that can be described by Eq. [10] through [25]. This example illustrates the point that a fractal porous medium is not restricted as to the shape of its solid matrix elements or its pores.

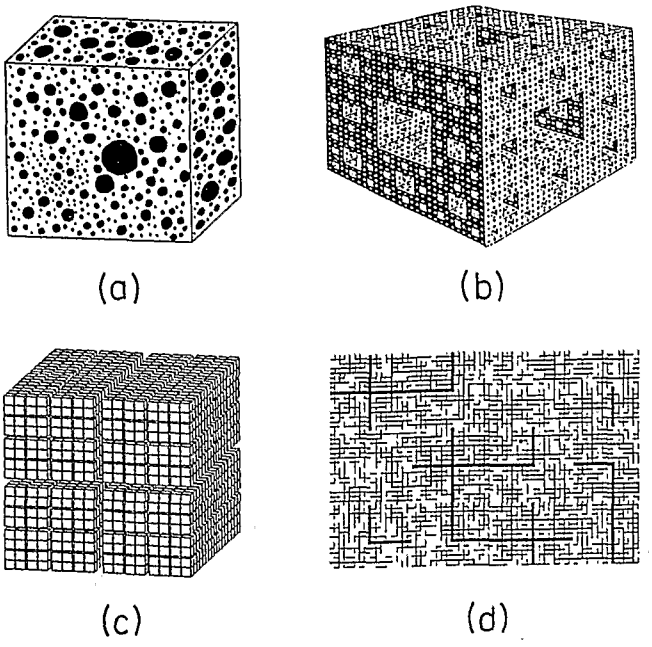

Fig. 1. Conceptual models of porous media: (a) a porous medium that is not necessarily fractal; (b) the Menger sponge (similarity ratio (r) = 1/3, N = 20, fractal dimension (D) = 2.7268), after Mandelbrot (1983, p. 145); (c) a completely fragmented fractal porous medium (r = 0.476, number of self-similar elements [N] = 8, D = 2.8); (d) cross-section of a random, incompletely fragmented fractal porous medium (r = 0.485, bulk fractal dimension (D_t) = 2.92, D = 2.87) showing active networks of fractures that are not crossed by larger fractures.

Figure 1c depicts an arrangement of pore space in a fractal medium that is quite different from the Menger sponge. The volume P_i now comprises pore elements that are distributed in a regular manner around the partial volumes V_{i+1} contained in the partial volume V_i. This arrangement represents a *fragmented fractal porous medium*: clusters of size-scaled, similar partial volumes separated from one another by a network of size-scaled, similar fractures. In this case, the solid matrix is a disconnected set, while the pore space remains a connected set. The latter is partitioned into virtual pore-size fractions in the usual way in order to bring out its self-similarity. The example shown in Fig.

1c is a three-dimensional analog of the well known Cantor dust (Mandelbrot, 1983, Ch. 8) for the case $r = 0.476$, $N = 8$, $D = 2.8$. The alternative choices, $r = 0.4665$, $N = 8$, or $r = 0.2986$, $N = 27$, would have resulted in fragmented, fractal porous media whose fractal dimension is the same as that of the Menger sponge in Fig. 1b. Equations [8] through [25] apply to these fractal media as well as to the Menger sponge: the connectedness of the solid matrix does not lead to quantitative characteristics differentiating fractal porous media.

The fragmented fractal porous medium is conceptually more similar to a natural soil, wherein aggregates of differing size can be associated with the partial volumes V_i. The pore space of soil consists of fractures or cracks that form ped boundaries and diminish the cohesiveness of the soil. The bulk element, of volume V_o, is any element that includes all sizes of fracture, such that no system of larger fractures separates bulk elements from one another. This element has the porosity ϕ and corresponding dry bulk density σ_o. The latter property is related to the solid mass M_o of the element by:

$$M_o = \sigma_o V_o \qquad [26]$$

An alternative expression to Eq. [26] is found by noting that the same mass of solid is contained in the aggregates of volume V_i at any step of fragmentation, i.e.,

$$M_o = N^i \sigma_i V_i \qquad (i = 0, \ldots, m) \qquad [27]$$

where σ_i is the bulk density of the partial volume V_i. As i increases from 0 to m, the partial volumes include less and less of the pore volume (cf. Fig. 1c), such that the density σ_i must increase to its limiting value σ_m in agreement with the implication of Eq. [18]. Indeed, Eq. [13], [26], and [27] can be combined to derive the relation

$$\sigma_i/\sigma_o = (1 - \Gamma)^{-i} \qquad (i = 0, \ldots, m) \qquad [28]$$

Given Eq. [8b] and [21], one can transform this equation into

$$\sigma_i/\sigma_o = (d_i/d_o)^{D-3} \qquad (i = 0, \ldots, m) \qquad [29]$$

Equation [29] is a well-known expression for the distribution of mass in a fractal object (Jullien and Botet, 1987, p. 31; Feder, 1988, p. 34). The density of a fractal porous medium decreases, as larger and larger component aggregates are considered, because larger and larger pores are thereby enclosed. If aggregates of differing size had the same bulk density σ_o, the fractal dimension of the medium would necessarily be 3 and its porosity would be zero, as follows from Eq. [24] and [29].

Incomplete Fragmentation

The fragmented, fractal porous medium is, in fact, merely a hypothetical construct, since, if every aggregate were to be surrounded by void space, the porous medium would collapse and the bulk volume would reduce to a collection of primary particles of size d_m. To ensure the stability of the pore space and structure, one must take into account the interaggregate bridges holding aggregates together. But these contacts will interrupt the fractures separating the aggregates. In other words, the fragmentation is not complete. In a fractal porous medium, this lack of complete fragmentation can be considered a scale-invariant property, expressed by the partitioning

$$V_o = FV_o + (1 - F)V_o \qquad (0 < F < 1) \qquad [30]$$

where F is a *clustering factor*. Following Turcotte (1986, 1989), we interpret F as the (uniform) probability that an element of volume will not fragment at a given fragmentation step. Thus the product FV_o is the portion of the volume V_o that remains unfragmented at the first step, whereas the portion $(1 - F)V_o$ is fragmented into aggregates of volume V_1. Following this approach, we can express the first step of incomplete fragmentation by

$$V_o = [FV_o + (1 - F)NV_1] + (1 - F)P_o \qquad [31]$$

which reduces to Eq. [11] with $i = 0$ when F vanishes. The first increment of pore volume, given by the second term on the right side of Eq. [31], can be rewritten in terms of V_o after combining Eq. [10] with the definition of the *reduced pore coefficient*:

$$\Gamma_r \equiv (1 - F)\Gamma \qquad (\Gamma_r < 1) \qquad [32]$$

The result is

$$(1 - F)P_o = \Gamma_r V_o \qquad [33]$$

so that Eq. [31] becomes

$$FV_o + (1 - F)NV_1 = (1 - \Gamma_r)V_o \qquad [34]$$

The next step of fragmentation will produce an increment of pore space $\Gamma_r(1 - \Gamma_r)V_o$ and a volume of aggregates $(1 - \Gamma_r)^2 V_o$, and so on. The porosity of an incompletely fragmented fractal porous medium is thus

$$\phi = 1 - (1 - \Gamma_r)^m \qquad [35]$$

and the partial porosity and corresponding bulk density of an aggregate are

$$\phi_i = 1 - (1 - \Gamma_r)^{m-i} \qquad (i = 0, \ldots, m - 1) \qquad [36a]$$

$$\sigma_i/\sigma_o = (1 - \Gamma_r)^{-i} \qquad (i = 0, \ldots, m) \qquad [36b]$$

These equations reduce to Eq. [16], [18], and [28] when F vanishes.

The physical significance of the clustering factor F can be understood as follows. We can express the volume of aggregates resulting from the $i-1$ step of incomplete fragmentation of a bulk soil element of volume V_o by

$$(1 - \Gamma_r)^i V_o = [F + (1 - F)(1 - \Gamma)]^i V_o \qquad [37]$$

The expansion of the right side of Eq. [37] involves the term $F^i V_o$, which represents the portion of the bulk soil element remaining unaffected by fragmentation. The other terms, which involve coefficients like $(1 - F)^k(1 - \Gamma)^l$, can be interpreted as volumes V_1 to V_i of aggregates of sizes d_1 to d_i. These aggregates are separated by fractures of size p_o to p_{i-1}. The ith step of fragmentation partitions, in proportion to $(1 - F)$, the volume denoted $F^i V_o$ by opening fractures of size p_i only. There will remain a volume $F^{i+1} V_o$, which will be, in turn, partially fragmented by fractures of opening p_{i+1} only, and so on. Thus, incomplete fragmen-

tation of a bulk soil element produces a complex fracture network, where $m - 1$ particular networks comprising single-size arrangements of fractures are embedded in a regular fractal network of fractures that does not extend throughout the bulk soil element. The single-size particular networks will be termed *active networks*. The volume of each active network is $\Gamma_r F^i V_o$, and the corresponding partial porosity is $\Gamma_r F^i$.

If some mechanical process completed the fragmentation, the result would be a collection of loose, self-similar aggregates scaled by the ratio r. In this totally fragmented porous medium, a pore coefficient can be defined as in Eq. [21]. But, considering Eq. [19] and [32], we hypothesize that the number of smaller aggregates contained in a larger one (by virtue of self-similarity) must be greater in an incompletely fragmented medium than in the completely fragmented medium. Consequentially, we shall write

$$\Gamma_r \equiv 1 - N_r r^3 \qquad [38]$$

where $N_r > N$ in Eq. [20]. The difference, $N_r - N$, characterizes the bridges bonding the aggregates in the actual porous-medium structure. Equation [38] leads to the definition of a *bulk fractal dimension*:

$$D_r \equiv \log N_r / \log(1/r) \qquad [39]$$

where $D_r > D$ in Eq. [19]. The fractal dimension of the completely fragmented porous medium represents both the fracture porosity of the actual medium and a complement of porosity obtained by the completion of fragmentation. The bulk fractal dimension, on the other hand, reflects only the porosity of the actual medium. From Eq. [38] and [39], the reduced pore coefficient may be expressed

$$\Gamma_r = 1 - r^{3-D_r} \qquad [40]$$

and Eq. [35] and [36] take the form

$$\phi = 1 - (d_m/d_o)^{3-D_r} \qquad [41]$$

$$\phi_i = 1 - (d_m/d_i)^{3-D_r} \qquad (i = 0, \ldots, m-1) \qquad [42a]$$

$$\sigma_i/\sigma_o = (d_i/d_o)^{D_r-3} \qquad (i = 0, \ldots, m) \qquad [42b]$$

which are analogous to Eq. [24], [25], and [29]. Finally, it follows from Eq. [21] and [40] that

$$F = \frac{r^{D-D_r} - 1}{r^{D-3} - 1} = 1 - \frac{\Gamma_r}{\Gamma} \qquad [43]$$

where D_r is the bulk fractal dimension of the actual porous medium and D is the fractal dimension of its aggregate distribution. As can be deduced from Eq. [43], the less completely developed is the fragmentation of the medium, the greater is the bulk fractal dimension D_r. Indeed, if a medium were not fragmented, the clustering factor would take on its maximum value: the condition $F = 1$ is equivalent to $D_r = 3$.

Aggregate-Size Distribution

Measurements of the aggregate-size distribution (Kemper and Rosenau, 1986) have long been used to characterize soil structure. In these measurements, as performed conventionally, for each size class represented by a mean (or median) diameter d_i, a certain mass $M(d_i)$ is measured that defines the contribution of the size class to the total sample distribution. Gardner (1956) has shown, in a study of more than 200 aggregate-size distributions for soils, that the distribution of $M(d_i)$ can be represented well by a lognormal function (Crow and Shimizu, 1988) whose independent variable is the ratio of the aggregate diameter to its median value.

The quantity $M(d_i)/d_i^3\sigma_i$, where σ_i is the average mass density of the aggregates with diameter d_i, is proportional to the number of aggregates in the size class i. (A geometric factor, dependent on aggregate shape, that ensures equality between $d_i^3\sigma_i$ and the average mass per aggregate has been omitted under the assumption that it is the same for all size classes.) Given the results of Gardner (1956) and Eq. [8b] and [29], the number of aggregates of size d_i in a fragmented fractal porous medium can be expressed in the form

$$\frac{M(d/d_i)}{d_i^3\sigma_i} = \frac{M(d/d_i)}{d_p^3\sigma_p}(d_i/d_p)^{-D} = \frac{M(r^{p-i}d/d_p)}{d_p^3\sigma_p}\, r^{(p-i)D} \qquad [44]$$

where Eq. [29] has been applied to the size classes i and p to derive the general equation

$$d_i^3\sigma_i = d_p^3\sigma_p(d_i/d_p)^D \qquad [45a]$$

and Eq. [8b] has been used recursively to yield the scaling relationship

$$d_i = r^{i-p}d_p \qquad [45b]$$

for any $p = 0, 1, \ldots, m-1$. Equation [44] represents the number distribution of aggregate diameters d in the size class i, as referenced to a particular size class p, via the scaling relationships that apply to a fractal porous medium (Eq. [8b] and [45]). In the simplest case, $M(d/d_i)$ is a rectangular "spike," centered on d_i and extending across the range of d values that is represented by the mean or median d_i (Gardner, 1956). In Eq. [44], $M(d/d_i)$ can be any mathematical function of d/d_i that encloses a finite area.

If the choice $p = m - 1, j \equiv p - i$ is made in Eq. [44], then the sum of terms over $j = 0, 1, \ldots, k$ has the form (dropping the constant factor $d_p^3\sigma_p$)

$$F_k(d/d_{m-1}) = M(d/d_{m-1}) + r^D M(rd/d_{m-1}) + \ldots + r^{kD}M(r^k d/d_{m-1}) \qquad [46]$$

The function $F_k(d/d_{m-1})$, is proportional to the number of aggregates with diameters less than d_{k+1} $(= r^{-(k+1)}d_{m-1})$, i.e., the conventional cumulative aggregate-size-distribution function. Another number-distribution function, related to F_k, is defined by the choice $p = 0$ in Eq. [44] (again dropping $d_p^3\sigma_p$):

$$N_k(d/d_o) = M(d/d_o) + r^{-D}M(r^{-1}d/d_o) + \ldots + r^{-kD}M(r^{-k}d/d_o) \qquad [47]$$

The function $N_k(d/d_o)$ is proportional to the number of aggregates with diameters larger than d_{k+1} $(= r^{k+1}d_o)$, i.e., the complement of the cumulative aggregate-size-distribution function. In Eq. [46], the first term on the right side is proportional to the number of smallest-size aggregates (class $m - 1$, see Eq. [1] and [8b]); the second term is proportional to the number of next-

smallest-size aggregates (diameter d_{m-1}/r), with the weighting factor r^D arising from the relationships in Eq. [45]; and so on. Each term after the first describes a scaling up of the smallest aggregate size to a new size via self-similarity, as expressed in Eq. [45]. In Eq. [47], the first term on the right side is proportional to the number of largest-size aggregates (Class 0); the second term is proportional to the number of next-largest size aggregates (diameter rd_o), with the weighting factor r^{-D}; and so on. Each term after the first in Eq. [47], as in Eq. [2] and [12], describes a scaling down of the largest aggregate size via self-similarity. In both Eq. [46] and [47], the number-distribution function defined reflects a fragmentation process in which aggregate size is amplified sequentially (cf. Montroll, 1987).

The dependence of $N_k(d/d_o)$ on d can be found after deriving a recursion relation for $N_k(rd/d_o)$:

$$\begin{aligned} N_k(rd/d_o) &= M(rd/d_o) + r^{-D}M(d/d_o) \\ &\quad + \ldots + r^{-kD}M(r^{-k+1}d/d_o) \\ &= r^{-D}[r^D M(rd/d_o) + M(d/d_o) \\ &\quad + r^{-D}M(r^{-1}d/d_o) \\ &\quad + \ldots + r^{(-k+1)D}M(r^{-k+1}d/d_o)] \end{aligned} \quad [48]$$

The second through the last terms in the square brackets in Eq. [48] are included in $N_k(d/d_o)$ (Eq. [47]), but a term in $M(r^{-k}d/d_o)$ is missing. After adding and subtracting this term in Eq. [48], the recursion relation is obtained:

$$\begin{aligned} N_k(rd/d_o) &= r^{-D}[N_k(d/d_o) + r^D M(rd/d_o) \\ &\quad - r^{-kD}M(r^{-k}d/d_o)] \end{aligned} \quad [49]$$

Since d_o is the largest aggregate size, $M(rd/d_o)$, corresponding to the diameter d_o/r, must be zero. The term in $M(r^{-k}d/d_o)$ does not vanish identically, but its domain is restricted to the range of d values that are represented by the smallest aggregate size d_k ($= r^k d_o$). The general behavior of $N_k(rd/d_o)$ thus will be controlled by the first term on the right side of Eq. [49]:

$$N_k(rd/d_o) = r^{-D}N_k(d/d_o) \quad [50]$$

This equation is satisfied by a power-law relationship (cf. Montroll, 1987):

$$N_k(d/d_o) = B_k(r)(d/d_o)^{-D} \quad [51]$$

as can be demonstrated by direct substitution into Eq. [50], where the function $B_k(r)$ is independent of d but may depend on r. Equation [51] is an aggregate-size number-distribution function for a fragmented fractal porous medium. Its dependence on the choice of reference diameter d_o is not essential, and the alternate form

$$N_k(d) = A_k(r)d^{-D} \quad [52]$$

where $A_k(r) \equiv B_k(r)d_o^D$, expresses the singular behavior of N_k in a way that can be tested experimentally. It follows from Eq. [52] that the graph of log $N(d_k)$ vs. log d_k should be approximately a straight line with slope equal to $-D$ for a fragmented fractal porous medium.

If Eq. [52] is applied to the aggregates in a soil that has been modeled as an incompletely fragmented fractal porous medium, a linear plot of log $N(d_k)$ vs. log d_k will lead to an estimate of the fractal dimension D instead of the bulk fractal dimension D_r. This is because D represents a completely fragmented fractal porous medium, and a soil whose aggregate-size distribution is being measured is merely a collection of aggregates resulting from the destruction of the structured soil. Indeed, if a nonporous solid (e.g., a piece of quartz) were fragmented by crushing it into a collection of scaled, self-similar particles, the particle-size distribution would obey Eq. [52] (approximately). Likewise, if an incompletely fragmented porous medium were crushed into fractal aggregates, their size distribution also would follow Eq. [52], even though the original porous medium would have the fractal dimension D_r.

WATER IN A FRAGMENTED FRACTAL POROUS MEDIUM

To simplify the mathematical description of water in a porous medium having a fragmented fractal structure, it will be assumed that the fracture walls are approximately parallel and that the fractures exhibit the same cross-section porosity in all directions, such that the hydraulic conductivity is a scalar quantity.

Water Content

Consider a fragmented fractal porous medium wherein the fractures of size $<p_{i-1}$ are filled with water by a capillary-flow process. The volume of water contained in the bulk volume V_o is equal to the sum of the successive pore-volume increments P_{m-1} to P_i. As implied in the discussion following Eq. [34], each of these pore-volume increments has the form $(1 - \Gamma_r)^j \Gamma_r V_o$ and the resulting volumetric water content is

$$\begin{aligned} \theta_i &= \sum_{j=i}^{m-1} \Gamma_r(1 - \Gamma_r)^j \\ &= (r^{3-D_r})^i - (r^{3-D_r})^m \end{aligned} \quad [53]$$

where the second step is derived after substitution of Eq. [40].

Water Potential

The pressure of water in a fracture ($\mathscr{P}_i$) must satisfy the Laplace equation:

$$\mathscr{P}_i = \gamma(1/R_1 + 1/R_2) \quad [54]$$

where γ is the liquid–vapor surface tension of water, R_1 is the radius of the meniscus curvature in a plane perpendicular to the fracture wall, and R_2 is the radius of the meniscus curvature in the plane of the fracture. If the lateral extension of the fracture is $\gg p_i$, R_2 can be assumed infinite and Eq. [54] becomes

$$\mathscr{P}_i = 2\gamma \cos\alpha/p_i \quad (i = 0, \ldots, m-1) \quad [55]$$

where α is the contact angle between liquid and solid. Assuming $\alpha = 0$ and expressing the pressure in meters of water, one derives an equation for the water potential in a fracture:

$$h_i = (2\gamma/\rho_w g)(1/p_i) \quad (i = 0, \ldots, m-1) \quad [56]$$

where ρ_w is the mass density of water and g is the gravitational acceleration. At 20 °C, $\gamma = 0.0727$ kg s^{-2}

and $\rho_w = 0.99823$ Mg m^{-3}. (Eq. [56] is identical to the well-known expression for the water pressure in a capillary tube of diameter $2p_i$.)

The general expression in Eq. [56] is specialized to a fragmented fractal porous medium by imposing a scaling relation on the fracture opening p_i. With repeated application of Eq. [8a], the water-potential expression becomes

$$h_i = h_o r^{-i} \qquad (i = 0, \ldots, m-1) \qquad [57]$$

where h_o is given by Eq. [56] for the case $i = 0$. Equation [57] expresses the fact that, in a fragmented fractal porous medium, the values of the water potential are scaled by r^{-i}, where i is a positive integer. In consequence, a plot of log (h_i/h_o) vs. an arbitrary integer scale will be a straight line of slope minus log r. Yet another form of Eq. [57] can be derived by introducing Eq. [35], [40], and [53]:

$$h_i = h_o[(1-\phi) + \theta_i]^{1/(D_r-3)} \qquad [58]$$

A log-log plot of this equation is a straight line with slope $1/(D_r - 3)$. Equations [57] and [58] can be tested with data on the moisture characteristic for an undisturbed soil, and linear plots of the transformed data permit the estimation of both the similarity ratio and the bulk fractal dimension.

Hydraulic Conductivity

The steady flow of water through fractures of a given opening p_j can be modeled by an integrated form of the Navier-Stokes equation (de Marsily, 1986):

$$q_{zj} = (d_o p_j)(p_j^2/12\mu)\{[(P_1 - P_2)/L] - \rho_w g\} \qquad [59]$$

where $d_o p_j$ represents the cross-sectional areas of vertically oriented (z axis) fractures of opening p_j and lateral extension d_o, μ is the kinematic viscosity of water (1.007×10^{-6} m^2 s^{-1} at 20 °C), L is the length of the fractures, and a pressure gradient is defined by P_1 at the top of the fracture and P_2 at the bottom, with $P_1 > P_2$. If unit area across a network of fractures of opening p_j contains n fracture cross-sections $d_o p_j$, its cross-section porosity is $\phi_{sj} = n d_o p_j$, and the total flow across this unit area is:

$$\begin{aligned} Q_{zj} &= n q_{zj} \\ &= n(d_o p_j)(p_j^2/12\mu)\{[(P_1 - P_2)/L] - \rho_w g\} \\ &= (\phi_{sj} p_j^2/12\mu)\{[(P_1 - P_2)/L] - \rho_w g\} \end{aligned} \qquad [60]$$

If the cross-sectional porosity is identical in all directions of space, Eq. [60] may be generalized to any direction of space, f:

$$Q_{fj} = -(1/12\mu)(\phi_{sj} p_j^2)[\text{grad } P + \rho_w g \text{ grad } z]_f \qquad [61]$$

where grad z is a vector with coordinates (0,0,1) (the z axis is vertical and oriented upwards) and $[\text{grad } P + \rho_w g \text{ grad } z]_f$ is the component of the total hydraulic gradient along the direction f. Assuming that the water is incompressible, we can introduce the hydraulic head, H:

$$H = (P\rho_w g) - z \qquad [62]$$

and Eq. [61] becomes:

$$Q_{fj} = -[(\rho_w g/12\mu)(\phi_{sj} p_j^2)][\text{grad } H]_f \qquad [63]$$

The general expression in Eq. [63] is specialized to a fragmented, fractal porous medium by modeling the cross-sectional porosity ϕ_{sj}. In a regular fractal network of fractures, every fracture of opening $p_i < p_o$ intersects a larger fracture. This fracture network, therefore, has zero hydraulic conductivity for any water content less than that at saturation. On the other hand, following the discussion of Eq. [37], we expect that, in an incompletely fragmented porous medium, there are $m - 1$ active networks of single-size fractures that are not crossed by larger fractures but are connected to the regular fractal network. This situation is illustrated in Fig. 1d for a random, incompletely fragmented fractal porous medium with similarity ratio $r = 0.485$ and $D_r = 2.92$, $D = 2.87$. If it is assumed that, at the water content θ_i.(Eq. [53]), fractures of opening $< p_{i-1}$ are filled with water, these active networks will have a nonzero hydraulic conductivity. Their cross-sectional porosity is the two-dimensional analog of the partial porosity $\Gamma_r F^i$ (see the discussion following Eq. [37]):

$$\phi_{si} \equiv \beta_r G^i \qquad [64]$$

where β_r is the two-dimensional analog of Γ_r and G is the analog of F.

Explicit expressions for β_r and G can be derived following the approach used to obtain Eq. [20] and [38], but with $V^{2/3}$, $N^{2/3}$, and $N_r^{2/3}$ replacing V, N, and N_r, respectively (area-to-volume ratio; cf. Turcotte [1989, p. 186]). The two-dimensional analog of Γ is

$$\begin{aligned} \beta &= [V_i^{2/3} - (NV_{i+1})^{2/3}]/V_i^{2/3} \\ &= 1 - (1-\Gamma)^{2/3} \\ &= 1 - (r^{3-D})^{2/3} \end{aligned} \qquad [65]$$

where the second step comes from Eq. [13] and the third from Eq. [21]. The corresponding two-dimensional analog of Γ_r is:

$$\beta_r = 1 - (1 - \Gamma_r)^{2/3} = 1 - (r^{3-D_r})^{2/3} \qquad [66]$$

The two-dimensional analog of F then follows:

$$G \equiv 1 - \frac{\beta_r}{\beta} = \frac{r^{2/3(D-D_r)} - 1}{r^{2/3(D-3)} - 1} \qquad [67]$$

If a uniform hydraulic gradient J_f is applied along a direction f, water will flow through a pore area of $\sum_{j=i}^{m-1} \phi_{sj}$ for each unit cross-sectional area perpendicular to the direction f. The flow rate may be expressed as

$$Q_f = \sum_{j=i}^{m-1} Q_{fj} \qquad [68]$$

where Q_{fj} is the flow per unit cross-sectional area produced by the hydraulic gradient J_f through the "active" network of fracture opening p_j, as given in Eq. [63]. Thus:

$$Q_f = -(\rho_w g/12\mu)(\beta_r \sum_{j=i}^{m-1} p_j^2 G^j)(\text{grad} H)_f \qquad [69]$$

and the hydraulic conductivity of the fracture system for the water content θ_i is

$$K_i = (\rho_w g/12\mu)(\beta_r \sum_{j=i}^{m-1} p_j^2 G^j) \quad [70]$$

Equation [70] shows that, in an incompletely fragmented, fractal porous medium, the hydraulic conductivity is compounded of the partial hydraulic conductivities of the active networks of fractures that are filled with water.

CONCLUDING REMARKS

The concepts developed here lead to a self-consistent description of a fractal porous medium that can be realized in nature. Scaling and self-similarity properties are imposed on both the pore space and the solid matrix, with the result that the porosity, bulk density, and aggregate-size distribution can be related to the mean (or median) aggregate diameters in successive partial volumes (Eq. [1]) of the porous medium. These relationships were derived first for a fractal porous medium in which the pore space is a connected set, while the solid matrix may be either connected (Fig. 1b) or not (Fig. 1c), the latter case being termed a (completely) fragmented fractal porous medium. The mathematical description of this kind of fractal porous medium is epitomized in Eq. [24], [25], [29], and [52], which relate the total porosity, the porosity and bulk density of a partial volume, and the aggregate-size distribution to aggregate diameter in terms of the fractal dimension of the medium, D. The equation derived for the total porosity shows that $D < 3$.

The completely fragmented fractal porous medium, however, cannot represent a soil in nature because every aggregate in it is surrounded by pore space, a situation that exists only for soil in the laboratory when collected for aggregate-size analysis. What is missing are the interaggregate bridges that cement aggregates together and endow natural soils with their field structures. These bridges occur because the fragmentation of the soil is not complete. Thus, it is necessary to define a probability of incomplete fragmentation (the clustering factor, F) and to incorporate it into the concept of a fractal porous medium. This can be done directly, if F has a uniform value for all partial volumes. The resulting expressions for the porosity and bulk density in terms of aggregate diameter (Eq. [41] and [42]) now involve the bulk fractal dimension of the medium, D_r. This latter parameter obeys the inequality $D < D_r < 3$. It represents the matrix and pore space of a medium that is not completely fragmented; i.e., D_r is the fractal dimension of the structured porous medium in nature and D is that of a collection of its aggregates.

Incomplete fragmentation produces a network of pores in which some are single-size fractures that are connected to the regular fractal network that does not extend throughout the porous medium (Fig. 1d). These single-size fractures are comprised in "active networks" that will exhibit a nonzero hydraulic conductivity when they are filled with water. At a given water content, defined by Eq. [53] for an incompletely fragmented fractal porous medium, the corresponding hydraulic conductivity can be expressed in terms of the similarity ratio and the fractal dimensions, D and D_r (Eq. [65], [66], and [70]). The moisture characteristic of the medium also can be expressed in terms of these parameters (Eq. [57] and [58]). Thus, the fractal concepts lead to a testable model of soil water properties. Very few data sets, however, are available with which to examine the applicability of Eq. [41], [42], [52], [57], [58], and [70] to natural soils. It is our hope that future research will provide the complete data on soil aggregate and soil water properties for undisturbed soils that will permit a conclusive test of the fractal model developed here.

ACKNOWLEDGMENTS

Gratitude is expressed by the senior author for the hospitality of the Department of Soil Science, University of California at Berkeley, during the tenure of a sabbatical leave from ORSTOM. Professors K. Loague and L.J. Waldron are thanked for their technical assistance and helpful advice during the preparation of this article, and Ms. Susan Durham and Ms. Joan Van Horn are thanked for their excellent typing of the manuscript.

REFERENCES

Arya, L.M., and J.F. Paris. 1981. A physico-empirical model to predict the soil moisture characteristic from particle-size distribution and bulk density data. Soil Sci. Soc. Am. J. 45:1023–1030.
Childs, E.C., and N. Collis-George. 1950. The permeability of porous materials. Proc. R. Soc. London 201A:392–405.
Cosby, B.J., G.M. Hornberger, R.B. Clapp, and T.R. Ginn. 1984. A statistical exploration of the relationships of soil moisture characteristics to the physical properties of soils. Water Resour. Res. 20:682–690.
Crow, E.L., and K. Shimizu. 1988. Lognormal distributions. Marcel Dekker, New York.
Danielson, R.E., and P.L. Sutherland. 1986. Porosity. p. 443–461. *In* A. Klute (ed.) Methods of soil analysis. Part 1. 2nd ed. Agron. Monogr. 9. ASA and SSSA, Madison, WI.
de Marsily, G. 1986. Quantitative hydrogeology: Groundwater hydrology for engineers. Academic Press, Orlando, FL.
Feder, J. 1988. Fractals. Plenum Press, New York.
Gardner, W.R. 1956. Representation of soil aggregate-size distribution by a logarithmic-normal distribution. Soil Sci. Soc. Am. J. 20:151–153.
Hartmann, W.K. 1969. Terrestrial, lunar and interplanetary rock fragmentation. Icarus 10:201–213.
Haverkamp, R., and J.Y. Parlange. 1986. Predicting the water-retention curve from particle size distribution: 1. Sandy soils without organic matter. Soil Sci. 142:325–339.
Hillel, D. 1980. Fundamentals of soil physics. Academic Press, New York.
Jullien, R., and R. Botet. 1987. Aggregation and fractal aggregates. World Scientific, Singapore.
Kemper, W.D., and R.C. Rosenau. 1986. Aggregate stability and size distribution. p. 425–442. *In* A. Klute (ed.) Methods of soil analysis. Part 1. 2nd ed. Agron. Monogr. 9. ASA and SSSA, Madison, WI.
Mandelbrot, B.B. 1983. The fractal geometry of nature. W.H. Freeman, San Francisco.
Montroll, E.W. 1987. On the dynamics and evolution of some sociotechnical systems. Bull. Am. Math. Soc. 16:1–46.
Saxton, K.E., W.J. Rawls, J.S. Romberger, and R.I. Papendick. 1986. Estimating generalized soil-water characteristics from texture. Soil Sci. Soc. Am. J. 50:1031–1036.
Schaefer, D.W. 1989. Polymers, fractals, and ceramic materials. Science (Washington, DC) 243:1023–1027.
Thompson, A.H., A.J. Katz, and C.E. Krohn. 1987. The microgeometry and transport properties of sedimentary rock. Adv. Phys. 36:625–694.
Turcotte, D.L. 1986. Fractals and fragmentation. J. Geophys. Res. 91:1921–1926.
Turcotte, D.L. 1989. Fractals in geology and geophysics. Pure Appl. Geophys. 131:171–196.
Tyler, S.W., and S.W. Wheatcraft. 1989. Application of fractal mathematics to soil water retention estimation. Soil Sci. Soc. Am. J. 53:987–996.
Tyler, S.W., and S.W. Wheatcraft. 1990. Fractal processes in soil water retention. Water Resour. Res. 26:1047–1054.

Fractal Fragmentation, Soil Porosity, and Soil Water Properties: II. Applications

Michel Rieu* and Garrison Sposito

ABSTRACT

The fractal model of Rieu and Sposito contains seven predictive equations that can be tested experimentally with data on aggregate characteristics and soil water properties for structured soils. However, data with which to test the model are extremely limited at present because of the need to have precise, concurrent measurements of aggregate physical properties (bulk density and size distribution) along with soil water properties for an undisturbed soil. For the five sets of suitable physical soil aggregate data currently available, good agreement was found with the fractal model bulk density–aggregate size and size-distribution relationships. For the single set of aggregate/soil water properties data available, good agreement also was found with the fractal model water-potential scaling relationship, moisture characteristic, and hydraulic conductivity–water content relationship. Model simulations of the last two soil water relationships for hypothetical sandy and clayey soils also were qualitatively accurate and showed the sensitivity of the model to the value of the fractal dimension. These encouraging results suggest that the model should have success in further experimental tests with natural soils.

THE CONCEPT of a fragmented fractal structure in a porous medium was developed by Rieu and Sposito (1991) to derive equations that relate porosity, bulk density, and aggregate size-distribution-characteristics of soil structure—as well as water content, water potential, and hydraulic conductivity—to fractal parameters such as the similarity ratio and the fractal dimension. The equations derived (see Appendix) are testable with suitable experimental data. We performed a limited testing of these equations with available data on aggregate porosity, bulk density, and size distribution, and with data on soil water properties.

MATERIALS AND METHODS

Aggregate Properties

Numerous studies of aggregate-size distribution have been carried out, as reported by Gardner (1956), but almost none includes other physical properties of aggregates, such as bulk density. An exception is the work of Chepil (1950), who compared three different methods of measurement of the bulk density of aggregates in three soils of differing texture. The results considered best by Chepil (1950) are reported in Table 1. Wittmus and Mazurak (1958) studied the aggregates in the Sharpsburg soil (fine, montmorillonitic, mesic Typic Argiudoll) and determined both their size distribution and bulk density. Their data are reported in Table 2. No other precise published data of this type were found in our search of the literature. For each soil, the mean diameter, d_i, of each size class i was computed (second column in Tables 1 and 2) along with the quantities d_i/d_o and σ_i/σ_o, where σ_i is the bulk density of the ith size class and σ_o is the bulk density of the largest aggregate. Straight lines were fitted to an experimental plot of log (σ_i/σ_o) vs. log(d_i/d_o) (see Eq. [A2]) for the four soils to estimate the bulk fractal dimension, D_r. A quantity proportional to the number of aggregates of each size class of the Sharpsburg soil, $N(d_i)$, was calculated with the equation:

$$N(d_i) = M(d_i)/(d_i^3\sigma_i) \qquad (i = 0, 1, \ldots.) \qquad [1]$$

where $M(d_i)$ is the mass of class i. The quantity log$[N(d_k)]$, where

$$N(d_k) = \sum_{i=0}^{k} N(d_i) \qquad [2]$$

was then plotted vs. log d_k (see Eq. [A3]) to estimate the fractal dimension, D, for the Sharpsburg soil.

Soil Water Properties

The fractal model of soil water properties was applied illustratively to physical data obtained by Bousnina (1984) for the surface horizon (0–0.2 m) of Ariana silty clay loam, collected from an experimental plot at the Institut National Agronomique de Tunis (Tunisia). These data are presented in Table 3. The soil bulk density was determined on undisturbed core samples of 10^{-4} m^3 volume and a pycnometer was used for the particle-density measurement. Aggregate separation was carried out by submerging undisturbed, large, dry clods in methanol, then drying and sieving (Braudeau, 1982). The elutriation methods, with Na hexametaphosphate as a dispersant, was used for mechanical analysis. The soil water retention curve (moisture characteristic) and hydraulic conductivity were determined at the field plot, for each layer of 0.2-m depth, by the method of zero-flow limit developed by Vachaud et al. (1981). A comparative determination of hydraulic conductivity (Table 3) was carried out from measurements of water potential and water content during the drainage of small, undisturbed cores using the laboratory method developed by Rieu (1978). No other complete set of physical data like these for a single soil was found in our review of the literature.

Values of the water potential in Table 3 were listed in ascending order and assigned to a set of increasing integer indices. The water potential (h) value of 0.22 m H_2O, measured at a maximum water content (θ_{max}) of 0.46 m^3 m^{-3}, was assumed to be the smallest value of the water potential in the Ariana soil; i.e.,

$$h_o = 0.22 \text{ m} \qquad [3]$$

The corresponding value of the fracture opening (p_o) was assumed to be the largest in the fractal length scale:

Table 1. Aggregate bulk densities in three soils of different texture (Chepil, 1950).

Size class	Mean size	Aggregate bulk density		
		Fine sandy loam	Silt loam	Clay
mm	mm	Mg m^{-3}		
6.40–2.00	4.200	1.49	1.42	1.49
2.00–1.19	1.595	1.58	1.58	1.68
1.19–0.84	1.025	1.75	1.68	1.70
0.84–0.59	0.715	1.82	1.61	1.73
0.59–0.42	0.505	1.94	1.72	1.75
0.42–0.25	0.335	2.17	1.75	1.80
0.25–0.15	0.200	2.11	1.82	1.75
0.15–0.10	0.125	2.15	2.10	1.80

M. Rieu, Centre ORSTOM Bondy, 70-74 Route d'Aulnay, 93143 Bondy Cédex, France; Garrison Sposito, Dep. of Soil Science, Univ. of California, Berkeley, CA 94720. Received 12 Feb. 1990. *Corresponding author.

Published in Soil Sci. Soc. Am. J. 55:1239–1244 (1991).

Table 2. Mass distribution and bulk density of aggregates of Sharpsburg soil (Wittmuss and Mazurak, 1958).

Size class	Mean size	Oversize mass	Aggregate density
mm	mm	kg	Mg m^{-3}
9.250–4.76	7.005	0.0177	1.320†
4.760–2.38	3.570	0.0063	1.373
2.380–1.19	1.785	0.0108	1.410
1.190–0.59	0.885	0.0188	1.480
0.590–0.297	0.446	0.0216	1.510
0.297–0.149	0.224	0.0138	1.540
0.149–0.074	0.111	0.0021	1.650
0.074–0.037	0.0555	0.0060	2.100
0.037–0.0185	0.02775	0.0025	2.360

† Extrapolated.

Table 3. Physical properties of the Ariana soil.

Aggregate-size distribution

Class number	Size class	Geometric mean size	Mass
	mm	mm	kg
0	2.00–1.60	1.79	0.01395
1	1.60–1.25	1.414	0.02100
2	1.25–1.00	1.118	0.01251
3	1.00–0.80	0.89	0.01040
4	0.80–0.63	0.71	0.00940
5	0.63–050	0.561	0.00637
6	0.50–0.315	0.400	0.00900
7	0.315–0.20	0.251	0.00720
8	0.20–0.10	0.141	0.00767
–	<0.10	–	0.00312

Soil water properties†

Water content	Water potential	Hydraulic conductivity
m^3 m^{-3}	m H_2O	m s^{-1}
0.460	0.22	4.44×10^{-5}
0.455	0.23	2.22×10^{-5}
0.451	0.26	1.11×10^{-5}
0.440	0.28	2.8×10^{-6}
0.431	0.32	1.1×10^{-6}
0.400	0.40	1.5×10^{-7}
0.384	0.50	5.8×10^{-8}
0.373	0.60	2.3×10^{-8}
0.362	0.70	2.5×10^{-8}
0.353	0.70	–
0.339	0.90	3.3×10^{-8}
0.333	0.95	–
0.330	0.98	2.5×10^{-8}
0.325	1.16	6.4×10^{-9}
0.333	0.95	–
0.287	1.66	–
0.258	2.00	–
0.258	2.30	–
0.243	2.34	–
0.238	2.40	–
0.234	2.50	–
0.221	2.80	–
0.215	3.10	–
0.209	3.24	–
0.205	4.20	–
0.186	5.80	–
0.180	6.20	–

Mechanical analysis

Size class	Mass
mm	kg
2.00–0.50	0.00140
0.50–0.05	0.01130
0.05–0.02	0.04430
0.02–0.002	0.02600
<0.02	0.01500
Bulk density:	1.409 Mg m^{-3}
Particle density:	2.610 Mg m^{-3}
Hydraulic conductivity:‡	$K(\theta) = 5.169 \times 10^{-5}\ \theta^{29.148}$ m s^{-1}

† Field measurement.
‡ Laboratory measurement.

$$p_o = 0.068 \text{ mm} \quad [4]$$

A plot of log (h_i/h_o) vs. the associated integer scale was then fitted to a straight line in order to estimate the similarity ratio (see Eq. [A4]). The porosity (ϕ) of the Ariana soil was calculated with the conventional formula (Danielson and Sutherland, 1986):

$$\phi = 1 - (\sigma_o/\sigma_m) \quad [5]$$

where σ_o is the bulk density and σ_m is the particle density given in Table 3. The aggregate-size distribution was calculated as described in Eq. [1] and [2], then plotted as log$[N(d_k)]$ vs. log d_k to test Eq. [A3] and estimate D. Measured values of the total porosity, water content, and water potential were plotted as log h vs. log $(1 - \phi + \theta)$ to test Eq. [A5] and estimate D_r.

RESULTS AND DISCUSSION

Bulk Density and Porosity

Figure 1 shows a log-log plot of σ_i/σ_o vs. d_i/d_o for the three sets of soil data in Table 1. The data show considerable scatter, but they are consistent in a statistical sense with Eq. [A2] as summarized in Table 4. The value of D_r, calculated by adding 3.00 to the value of the slope of each line determined by linear regression, fell in the range 2.88 to 2.95.

The plot of log(σ_i/σ_o) vs. log(d_i/d_o) for the Sharpsburg soil (Fig. 2) showed a clear break around the aggregate-size value $d_i = 0.111$ mm, which corresponds to the size class 0.149 to 0.074 mm in Table 2. As pointed out by Wittmus and Mazurak (1958), the aggregates of <0.074-mm size contained more sand and silt than did the larger aggregates. The density of their primary particles is thus greater and their porosity is coarser. These physical differences support the existence of two separate fragmented fractal structures through the range of aggregate sizes. (Indeed, the aggregates of < 0.074-mm size may well have a different shape, since they comprise a sandy skeleton on which the flocculation of clay develops larger aggregates.) In order to examine this possibility in more detail, Eq. [A2] was applied to two separate ranges of size class: between the mean limits $d_{o1} = 7.005$ mm, $d_{m1} = 0.111$ mm, and between $d_{m1} = 0.111$ mm and $d_{m2} = 0.02775$ mm. Two straight lines were fitted, resulting in fractal dimensions of 2.95 and 2.74, respectively (Table 5). The smaller value of the second fractal dimension can be interpreted as a reflection of a more fragmented structure, consistent with the physical properties of the second size-class range.

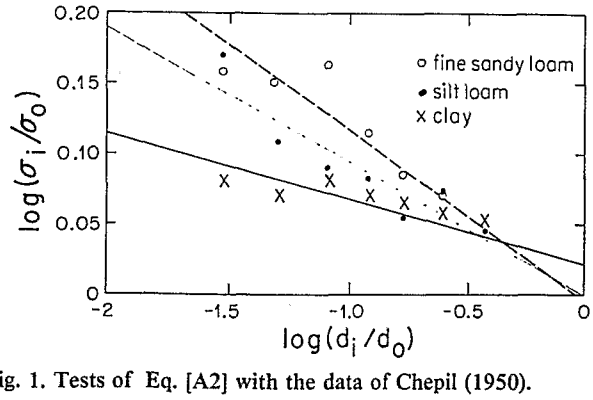

Fig. 1. Tests of Eq. [A2] with the data of Chepil (1950).

Table 4. Parameters resulting from linear regression of log (σ_i/σ_o) vs. log(d_i/d_o),where σ_i is the bulk density of the ith aggregate size class, σ_o is the bulk density of the largest aggregate, d_i is the mean diameter of the ith size class, and d_o is the diameter of the largest aggregate, based on the data of Chepil (1950).

Soil	Slope	Intercept	r^2	Level of Significance	Fractal dimension
Fine sandy loam	−0.1199	−0.0037	0.92	$P < 0.001$	2.88
Silt loam	−0.0950	−0.001	0.90	$P < 0.001$	2.91
Clay	−0.0469	0.021	0.78	$P < 0.01$	2.95

The existence of two fragmented fractal structures in the Sharpsburg soil can be tested further by modeling the porosity of its aggregates. The experimental values of this parameter were calculated by applying Eq. [5], with σ_o replaced by an aggregate bulk density (Table 2) and σ_m set equal to the largest bulk density of the aggregates (i.e., $\sigma_m \equiv \sigma_{m2} = 2.36$ Mg m^{-3}). A model of the aggregate porosity was developed by rewriting Eq. [5] in the form

$$\phi = 1 - (\sigma_o/\sigma_{m1})(\sigma_{m1}/\sigma_{m2})$$
$$= 1 - (d_o/d_{m1})^{3-D_{r1}}(d_{m1}/d_{m2})^{3-D_{r2}} \quad [6]$$

where the second step comes from substituting Eq. [A2]. Equation [A2] can be extended to describe the porosity of an arbitrary aggregate by writing it in the form:

$$\phi(d,d') = 1 - (d/d_{m1})^{3-D_{r1}}(d'/d_{m2})^{3-D_{r2}} \quad [7]$$

where $d = d_{m1}$ while $d_{m2} \leq d' \leq d_{m1}$ and $d' = d_{m1}$ while $d_{m1} \leq d \leq d_o$. The values of d_{m1}, d_{m2}, D_{r1}, and D_{r2} are available from Table 5. A plot of the resulting $\phi(d,d')$ vs. aggregate size is shown in Fig. 3 along with the experimental aggregate porosity values. The agreement between Eq. [7] and the data is very good, showing that the hypothesis of two embedded fractals is consistent with the observed porosity of the Sharpsburg soil.

Aggregate-Size Distribution

Figure 4 shows a log-log plot of $N(d_k)$ vs. d_k for the Sharpsburg soil (data from Table 2 were used in Eq.

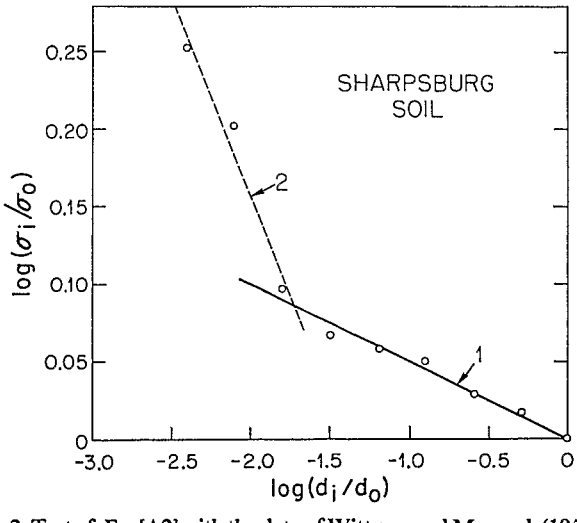

Fig. 2. Test of Eq. [A2] with the data of Wittmus and Mazurak (1958), indicating two embedded fractal structures (Lines 1 and 2).

Table 5. Parameters resulting from statistical fitting of the Sharpsburg soil data (Table 2) to Eq. [A2] or [A3].

	7.005–0.111 mm		0.111–0.02775 mm	
	Eq. [A2]	Eq. [A3]	Eq. [A2]	Eq. [A3]
Slope	−0.04998	−2.842	−0.25748	−2.581
r^2	0.98	0.98	0.96	0.98
Level of significance	P <0.001	P<0.001	P<0.02	P<0.01
Fractal dimension	2.95	2.84	2.74	2.58

[1] and [2]). Again, confirming the "embedded fractal" hypothesis, an apparent break was noted near the diameter of 0.111 mm. Two lines thus were fitted to the experimental points corresponding to the size ranges greater and less than 0.111 mm, respectively. The observed aggregate-size distribution satisfies Eq. [A3] fairly well when applied piecewise. The corresponding fractal dimensions were slightly smaller than those determined from Eq. [A2]: 2.84 instead of 2.95 for the size range 7.005 to 0.111 mm, and 2.58 instead of 2.74 for the smaller size range (Table 5). These differences are not unexpected; as suggested by Rieu and Sposito (1991), D determined from Eq. [A3] reflects the mechanical destruction of the incompletely fragmented structure of a soil. The value of this latter dimension

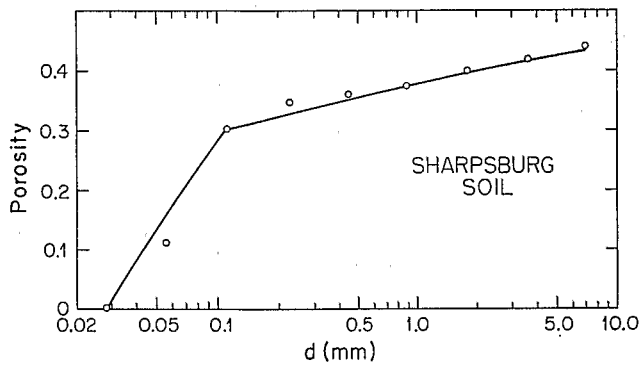

Fig. 3. Test of Eq. [7] with aggregate porosities computed using the bulk-density data for the Sharpsburg soil (Table 2).

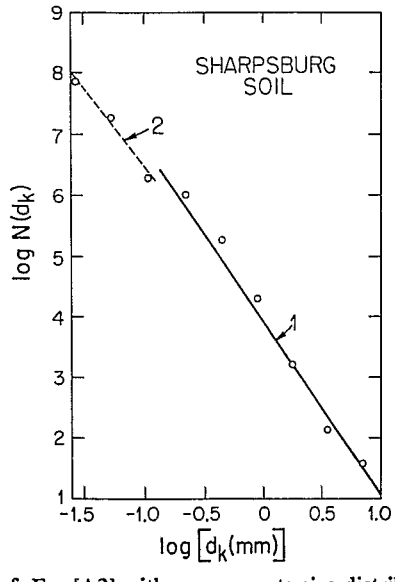

Fig. 4. Test of Eq. [A3] with an aggregate-size distribution calculated with the data for the Sharpsburg soil (Table 2).

Table 6. Fractal parameters for the Ariana and hypothetical sandy and clayey soils.

Property	Symbol	Ariana	Sandy soil	Clayey soil
Bulk density (Mg m^{-3})	σ_o	1.409	1.41	1.416
Particle density (Mg m^{-3})	σ_m	2.61	2.61	2.61
Similarity ratio	r	0.82	0.82	0.82
Clustering factor	F	0.418	0.418	0.418
Bulk fractal dimension	D_r	2.90	2.88	2.95
Fractal dimension	D	2.83	2.79	2.91
Fracture opening (mm)	p_o	0.068	0.081	0.034
Fragmentation number	m	31	26	62
Reduced pore coefficient	Γ_r	0.01965	0.02353	0.0099

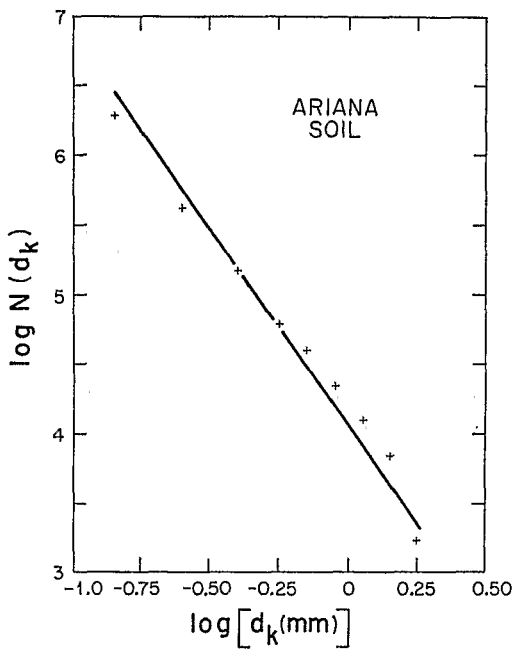

Fig. 5. Test of Eq. [A3] with the aggregate-size distribution for the Ariana soil.

is expected to be smaller than D_r determined from Eq. [A2]. The difference, $D_r - D$, expresses the decrease in fractal dimension resulting from the completion of fragmentation.

Figure 5 shows a log-log plot of $N(d_k)$ vs. d_k for the Ariana soil, based on data in Table 3 and Eq. [1] and [2]. (The values of σ_i needed in Eq. [1] were calculated with Eq. [A2] and the value of D_r determined from an analysis of the moisture-characteristic data, as described below.) The slope of the line through the data points, fit by linear regression ($r^2 = 0.97$*** [significant at $P = 0.001$]), led to $D = 2.83$, according to Eq. [A3].

Soil Water Properties

Figure 6 shows a graph of log (h_i/h_o) vs. size class i for the Ariana soil using the water-potential data in Table 3 and h_o given by Eq. [3]. The conformity of the data to a straight line was excellent ($r^2 = 0.996$***) and the slope value led to a similarity ratio $r = 0.8209$ according to Eq. [A4]. With the value of ϕ computed from Eq. [5], the measured values of the water potential and water content were plotted according to Eq. [A5], as shown in Fig. 7. Linear regression of the data ($r^2 = 0.991$***) yielded a slope equal to -9.5591 and

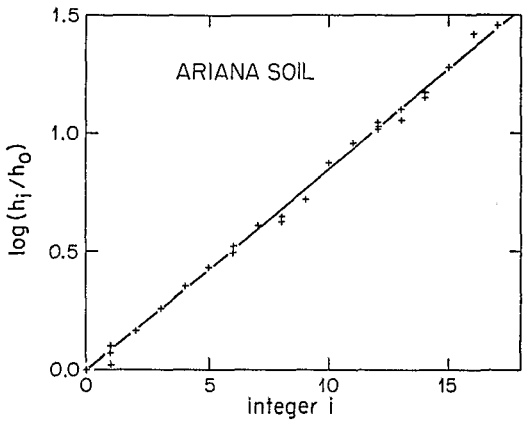

Fig. 6. Test of Eq. [A4] with water-potential data for the Ariana soil (Table 3).

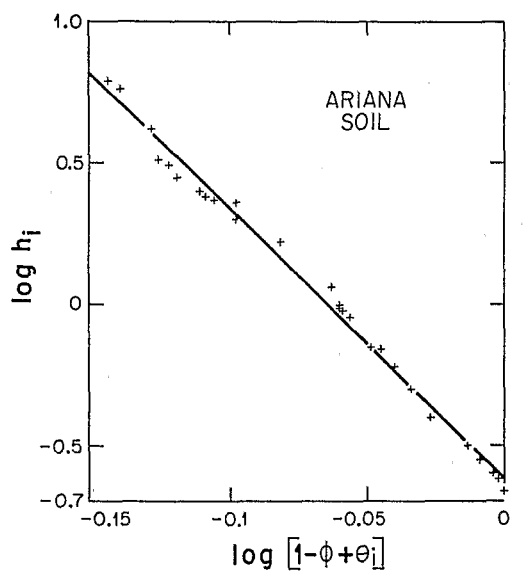

Fig. 7. Test of Eq. [A5] with water-retention data for the Ariana soil (Table 3).

a corresponding $D_r = 2.90$. This latter value is larger than D (= 2.83), indicating the lesser extent of fragmentation of the undisturbed field soil. Given Eq. [A1] for the case $i = 0$ and the relation $d_m/d_o = r^m$ (Rieu and Sposito, 1991, Eq. [23]), the value of the exponent m can be calculated, with the result $m = 31$. The fractal parameters for the Ariana soil are summarized in Table 6.

Given the physical parameters in Table 3 and the fractal parameters summarized in the third column of Table 6, the values of the parameters Γ, Γ_r, and clustering factor, F, can be calculated with formulas derived by Rieu and Sposito (1991, Eq. [21], [40], and [43]):

$$\Gamma = 0.03375 \qquad \Gamma_r = 0.01965 \qquad F = 0.418 \quad [8]$$

and the corresponding cross-section parameters required to model the hydraulic conductivity can be computed (Rieu and Sposito, 1991, Eq. [65]–[67]):

$$\beta = 0.0226 \qquad \beta_r = 0.01313 \qquad G = 0.419 \quad [9]$$

The parameters in Eq. [9] can be used in Eq. [A6]. For successive values of the increment i, $(0 \leq i \leq m -$

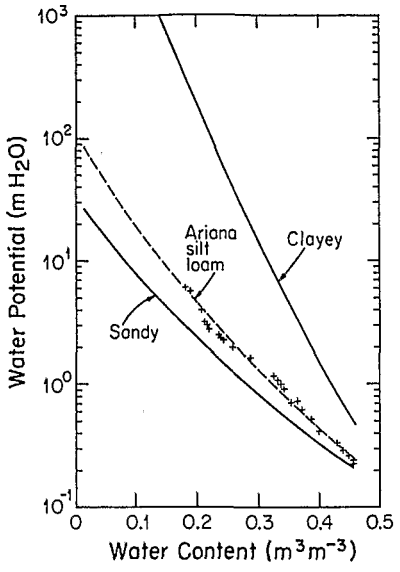

Fig. 8. Test of Eq. [A5] and [A7] with water-retention data for the Ariana soil and hypothetical moisture characteristics for fractal sandy and clayey soils in Table 6.

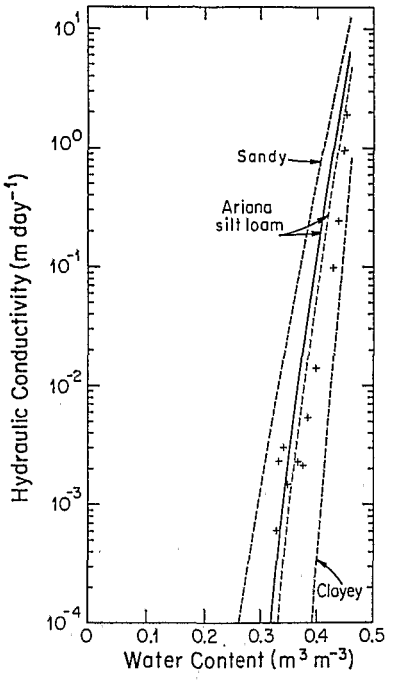

Fig. 9. Test of Eq. [A6] and [A7] with hydraulic-conductivity data for the Ariana soil (dashed line) and hypothetical hydraulic-conductivity curves for fractal sandy and clayey soils based on the parameters in Table 6. The solid line associated with the Ariana soil is a plot of the laboratory-based relation for hydraulic conductivity (Table 3).

1), the soil water content was calculated with Eq. [A7], the water potential with Eq. [A5], and the hydraulic conductivity with Eq. [A6]. The results are compared with experimental values taken from Table 3 in Fig. 8 and 9. The excellent agreement between the model equations and experiment in Fig. 8 and the good agreement in Fig. 9 suggest that the concept of an incompletely fragmented fractal porous medium is consistent with the structure of the Ariana soil. It is possible that the somewhat poorer agreement between the model and data in Fig. 9 results both from lesser precision in the conductivity measurements than in the matric-potential measurements and from a likely greater sensitivity of the conductivity to the nonfractal structure in a porous medium.

The sensitivity of the model to the fractal parameters was examined by repeating the calculation above using different fractal dimensions under the assumption of constant similarity ratio, r, F, and ϕ. Values of $D_r = 2.88$ and $D_r = 2.95$ were determined for sandy and clayey soils, respectively, in Table 1, whereas the Ariana soil (silty clay loam) has an intermediate value of 2.90. Fractal fragmented models of hypothetical sandy and clayey soil structures thus can be developed with the Ariana soil as a reference (Table 6). The value of D was calculated with Eq. [43] in Rieu and Sposito (1991) and the exponent m was calculated with Eq. [A1] following the method used to compute this parameter for the Ariana soil. Since the parameter Γ_r can be interpreted physically as the partial porosity contributed by pores of a given size (Rieu and Sposito, 1991, Eq. [35]), the fracture opening p_o should scale with Γ_r:

$$p_o'/p_o = \Gamma_r'/\Gamma_r \qquad [10]$$

Equation [10] was used to calculate p_o values for the sandy and clayey soils with Γ_r and p_o (Eq. [4] and [8]) for the Ariana soil taken as a reference. The resulting model relations between water content, water potential, and hydraulic conductivity are presented in Fig. 8 and 9. The models of water potential and hydraulic conductivity are seen to be rather sensitive to the value of the fractal dimension. It should be noted also that the shapes of the model curves are consistent with conventional experimental results for sandy and clayey soils (Hillel, 1980, p. 150), indicating the ability of Eq. [A5] to [A7] to describe fundamental soil water properties.

CONCLUSIONS

The fractal model of a soil developed by Rieu and Sposito (1991) is accessible to experiment through the seven equations in the Appendix. Equations [A1] to [A3] express three physical properties that characterize a fragmented fractal porous medium: decreasing aggregate bulk density with increasing aggregate size, a power-law aggregate-size distribution, and incomplete fractal fragmentation, which is reflected in the difference between D and D_r. The corresponding soil water properties are expressed by Eq. [A4] to [A7]: a water potential that scales in inverse powers of the similarity ratio and whose dependence on water content is expressed by a power-law relationship with an exponent equal to the inverse of the difference between the bulk fractal dimension and the Euclidian dimension; for a given water content, a hydraulic conductivity that is the sum of partial hydraulic conductivities contributed by the active single-size arrangements of fractures that are water filled. Very few experimental data are available with which to test these equations.

The limited comparisons of Eq. [A1] through [A7] with experimental measurements, illustrated in Fig. 1 through 9, suggest that aggregates in soils may be frac-

tal objects and that the pore space in undisturbed soils may exhibit structure characteristic of an incompletely fragmented fractal medium. Precise data on soil aggregate physical properties and soil water parameters, taken concurrently, will be required in order to evaluate the applicability of fractal concepts to soils.

ACKNOWLEDGMENTS

Gratitude is expressed by the senior author for the hospitality of the Department of Soil Science, University of California at Berkeley, during the tenure of a sabbatical leave from ORSTOM. Professors K. Loague and L.J. Waldron are thanked for their technical assistance and helpful advice during the preparation of this article, Ms. Susan Durham and Ms. Joan Van Horn are thanked for their excellent typing of the manuscript, and Mr. Frank Murillo is thanked for preparation of the figures.

APPENDIX

Equations describing a fragmented fractal porous medium, derived by Rieu and Sposito (1991), where i is an integer index running from 0 to m.

Porosity: $\phi_i = 1 - (d_m/d_i)^{3 - D_r}$ [A1]

Bulk density: $\sigma_i/\sigma_o = (d_i/d_o)^{D_r - 3}$ [A2]

Aggregate size distribution: $N_k(d) = A_k(r)d^{-D}$ [A3]

Scaled water potential: $h_i = h_o r^{-i}$ [A4]

Water-retention curve: $h_i = h_o[(1 - \phi) + \theta_i]^{1/(D_r - 3)}$ [A5]

Hydraulic conductivity: $K_i = (\rho_w g/12\mu)(\beta_r \sum_{j=i}^{m-1} p_j^2 G^j)$ [A6]

Water content: $\theta_i = (r^{3 - D_r})^i - (r^{3-D_r})^m$ [A7]

REFERENCES

Bousnina, H. 1984. Comparaison de differentes méthodes d'étude des propriétés hydrodynamiques d'un sol à texture fine. Mém. Fin. Et. Institut National Agronomique. Tunis, Tunisia.

Braudeau, E. 1982. Fractionnement physique du sol. Méthode de séparation et étude de comportement d'agrégats de 0.050 à 2 mm. Cah. ORSTOM Sér. Pédol. 19:353–367.

Chepil, W.S. 1950. Methods of estimating apparent density of discrete soil grains and aggregates. Soil Sci. 70:351–362.

Danielson, R.E., and P.L. Sutherland. 1986. Porosity. p. 443–461. *In* A. Klute (ed.) Methods of soil analysis. Part 1. 2nd ed. Agron. Monogr. 9. ASA and SSSA, Madison, WI.

Gardner, W.R. 1956. Representation of soil aggregate-size distribution by a logarithmic-normal distribution. Soil Sci. Soc. Am. Proc. 20:151–153.

Hillel, D. 1980. Fundamentals of soil physics. Academic Press, New York.

Rieu, M. 1978. Eléments d'un modèle mathematique de prédiction de la salure dan les sols irrigués. Application aux polders du Tchad. Thès. Spéc. Univ. P. Sabatier, Toulouse, France.

Rieu, M., and G. Sposito. 1991. Fractal fragmentation, soil porosity, and soil water properties: I. Theory. Soil Sci. Soc. Am. J. 55:1231–1238 (this issue).

Vachaud, G., M. Vauclin, and J. Colombani. 1981. Bilan hydrique dans le Sud Tunisien: I. Caractérisation expérimentale des transferts dans la zone non-saturée. J. Hydrol. (Amsterdam) 49:31–52.

Wittmus, H.D., and A.P. Mazurak. 1958. Physical and chemical properties of soil aggregates in a Brunizem soil. Soil Sci. Soc. Am. Proc. 22:1–5.

Equivalent Diameter of Simulated Macropore Systems during Saturated Flow

G. H. Dunn* and R. E. Phillips

ABSTRACT

Under natural conditions, soil pore systems that conduct water vary in shape, cross-sectional area, and continuity. Because of this, it is virtually impossible to predict the flow of water through these pore systems. We conducted an experiment to measure the equivalent spherical diameter, d_{eq}, of simulated nonuniform macropore systems for 11 combinations of lengths of three radii of cylindrical, straight-walled glass tubing during saturated flow. Also, we wanted to determine if experimental data of d_{eq} of the simulated macropores are described by a derived theoretical equation where d_{eq} is a function of the total length of the three tubes, their individual lengths, and their radii. Three known, uniform-i.-d. tubes of differing lengths, of cylindrical, straight-walled glass, in series configuration were used to simulate to a small degree the geometry of macropores as they occur in the field. Inside diameters were 5.08 (L), 1.88 (M), and 0.94 (S) mm. A constant length of 0.60 m was maintained for the pore system. The d_{eq} values of these non-uniform pore systems were measured. Flux values were measured at eight hydraulic pressures. Equivalent diameters were calculated using Poiseuille's law from the measured flux. The data points of d_{eq} of the pore system were described well by the derived equation. The experimental saturated hydraulic conductivity (K_{sat}) was also well described by a derived function.

Dep. of Agronomy, Univ. of Kentucky, Lexington, KY 40546-0091. Contribution from the Kentucky Agric. Exp. Stn. as Journal no. 90-3-108. Received 11 June 1990. *Corresponding author.

Published in Soil Sci. Soc. Am. J. 55:1244–1248 (1991).

SEVERAL RESEARCHERS have proposed various means of characterizing the size distribution of micropores in soil. Marshall (1958) developed a relationship between intrinsic permeability and size distribution of pores from moisture-release curves. However, Marshall's method involved micropores smaller than 0.2-mm equivalent diameter. Cary and Hayden (1973) also used moisture-release curves to calculate an index of pore-size distribution of pores >0.002-mm equivalent diameter. Wilkins et al. (1977) developed a laboratory technique to characterize pore size by intruding a fluorescent resin, sectioning samples, and taking photographs under a black light.

The development of the tension infiltrometer (Dixon, 1975; Diriksen, 1975; Clothier and White, 1981; White and Perroux, 1987) has enabled the measurement and distribution of the equivalent diameter of macropores in the field (Watson and Luxmoore, 1986; Wilson and Luxmoore, 1988; Ankeny et al., 1988). However, the measurement and distribution of macropores using the tension infiltrometer does not enable calculation of the equivalent diameters of macropores as a function of differing macropore geometries. The equivalent diameter of macropores will be the same for many combinations of varying lengths and cross-sectional areas within macropores.

As far as can be determined, equivalent diameter of